Phosphazene Based Additives for Improvement of Safety and Battery Lifetimes in Lithium-Ion Batteries

220th Meeting of the Electrochemical Society

Mason K. Harrup
Kevin L. Gering
Harry W. Rollins
Sergiy V Sazhin
Michael T. Benson
David K. Jamison
Christopher J. Michelbacher
Thomas A. Luther

October 2011

Idaho National Laboratory

Phosphazene Based Additives for Improvement of Safety and Battery Lifetimes in Lithium-Ion Batteries

Mason K. Harrup, Kevin L. Gering, Harry W. Rollins, Sergiy V. Sazhin, Michael T. Benson, David K. Jamison, Christopher J. Michelbacher, Thomas A. Luther

Idaho National Laboratory Idaho Falls, ID 83415, USA

There needs to be significant improvements made in lithium-ion battery technology principally in the areas of safety and useful lifetimes to truly enable widespread adoption of large format batteries for the electrification of the light transportation fleet. In order to effect the transition to lithium ion technology in a timely fashion, one promising next step is through improvements to the electrolyte in the form of novel additives that simultaneously improve safety and useful lifetimes without impairing performance characteristics over wide temperature and duty cycle ranges. Recent efforts in our laboratory have been focused on the development of such additives. This paper presents the results of the study of a series of structurally similar phosphazenes that exhibit promise for use as electrolyte additives. This series, termed the SM series, employs cyclic phosphazene trimers with six pendant groups each composed of short chain linear ethers.

Introduction

The current generation of lithium ion batteries is in widespread use for a broad range of mobile power needs. However, there still remain significant challenges that must be addressed in order to move lithium ion technology into larger format applications, such as vehicle technologies and stationary power. Chief among these is safety concerns of the electrolyte. As most commercial electrolytes employ $LiPF_6$ as the lithium salt dissolved in a mixture of organic carbonates and/or esters (1) this mix brings several intrinsic problems. These solvents are highly volatile as well as highly flammable. Also, they and their combustion products can be toxic. This presents a serious safety problem in situations where the battery is under abuse or if the battery casing is compromised. While this concern is partially mitigated in very small cells such as those that power small electronics, the problem rapidly grows in magnitude as battery sizes grow. In order to realize larger format batteries, this problem must be addressed.

The search for alternative solvents to serve as replacements for the current generation of electrolyte solvents has received such attention in recent years. Approaches under study include the use of sulfones (2) and most recently ionic liquids (3). However it may be some time into the future before carbonates and esters may be entirely replaced. As a practical interim strategy, it has been recognized that improvements in the performance and safety record of the current generation of electrolytes may be realized through the use of additives. (4) Additives have been the subject of research since the early 1990's (5) and is a topic of rapidly growing interest, especially in the past few years. Research into

additives has taken several forms to address various challenges in lithium ion batteries. Some have employed additives to improve SEI formation (6), overcharge protection (7), and flammability suppression. (8) Others have employed additives not as co-solvents but rather through the use of novel salts to achieve improved thermal stability. (9) This work reports on the behavior of novel liquid phosphazene-based additives for lithium ion batteries.

Experimental

Instrumentation

All NMR analyses were performed on a Bruker DMX 300WB spectrometer. Viscometry measurements were performed using a Cambridge DL-4100 (falling bob) viscometer, in an argon glovebox, the data presented is the average of 3 individual measurements. Conductivity measurements were performed using a TOA CM-30R conductivity meter in an argon glovebox, the data presented is the average of 10 individual measurements. Flash point determinations were performed using a Setaflash 82000-0 (electric ignition) using a ramp determination method, the data reported is the average of 3 individual determinations, all with fresh sample. Trace water determinations were performed on a Mettler Toledo C30 Karl Fischer coulometer (in an argon glovebox), the data presented is the average of 3 individual measurements. Electrochemical measurements were made On a Solaratron SI 1260 impedance/phase gain analyzer with a Solaratron SI 1287 electrochemical interface. Coin cells were tested using a Maccor Series 4000 5V/5A full range tester. Thermal stability experiments were run in an ESPEC BTU133 thermal chamber.

Reagents

Hexachlorocyclotriphosphazene was obtained from Molport.com and was purified via sublimation immediately prior to use. All pendant groups were obtained from Aldrich Chemical Company, diethleneglycolmonomethyl ether and monoethyleneglycolmonomethyl ether were distilled and stored in Sure-Seal containers prior to use. Isopropanol and ethanol were obtained as anhydrous grade and used as received. Sodium metal was obtained from Aldrich Chemical Company and the kerosene washed with hexanes and blotted dry with a laboratory wipe before use. Sodium hydride (95%, dry) was obtained from Aldrich Chemical Company and used as received. 1,4-Dioxane and tetrahydrofuran were obtained from Aldrich Chemical Company as anhydrous grade and used as received. Dichloromethane was obtained from Aldrich Chemical Company and used as received. Nanopure water (18.4 M Ω-cm) was generated in the laboratory using a Barnstead NANOpure II water purification system. The baseline electrolyte was purchased from the Osaka Chemical Company, "Chameleon Reagent" EC:EMC 2:8 (v/v%), 1.2 M $LiPF_6$, opened only in an argon glovebox and used as received.

Synthesis of the Additives

Synthesis of all of the additives followed very similar synthetic pathways all employing Schlenk techniques. The specific formulation described here is for the

synthesis of SM-2. Sodium hydride (18.18g, 720 mmol) was placed into an oven dried 2 L three-neck flask fitted with a reflux condenser, a dry nitrogen inlet, and a septum stopper. The dry nitrogen outlet issued from the top of the reflux condenser into an oil bubbler apparatus charged with approximately two inches of silicon oil. 1,4-Dioxane (700ml) was cannulated into the flask and the reaction was stirred using a magnetic stirbar. Anhydrous monoethyleneglycolmonomethyl ether (56.97g, 749mmol) was cannulated into the reaction vessel and the reaction warmed with a heating mantle to a gentle reflux overnight.   The reaction was returned to room temperature. Hexachlorocyclotriphosphazene (50.0 g, 144 mmol) was placed in a 500 ml oven dried round bottomed flask fitted with a septum stopper. 1,4-Dioxane (200 ml) was cannulated in and the solution stirred magnetically. After dissolution was complete, the trimer solution was cannulated into the alkoxide reaction solution. The reaction was brought to a gentle reflux and reaction progress was monitored by ^{31}P NMR until it was determined that the reaction was complete, which took approximately two hours. In a separate oven dried 1 L three neck flask outfitted as described above was placed sodium hydride (7.27g, 288 mmol) along with anhydrous 1,4-dioxane (400 ml) and the reaction stirred magnetically. Anhydrous ethanol (13.25g, 288 mmol) was added via syringe. The reaction was allowed to proceed at room temperature for 30 minutes. This reaction mixture was added to the main reaction and the mix heated to a gentle reflux for two hours. Completion of the reaction was confirmed by ^{31}P NMR and the reaction was cooled to room temperature. The excess nucleophile was quenched with 250 ml of water and brought to neutral pH with 2.0 M HCl. The volume of the reaction mixture was reduced on a rotary evaporator to a final volume of 300 ml. This solution was transferred to a 2 L separatory funnel and 500 ml of dichloromethane was added, forming two phases. These were separated and the dichloromethane phase was retained. This was returned to the separatory funnel where it was subsequently washed seven times with fresh aliquots of nanopure water (500 ml each). The final product was obtained by the removal of the dichloromethane solvent by rotary evaporation to yield a clear, colorless oil. The oil was dried in a vacuum/argon oven at 85 °C, 25 mTorr Ar for a minimum of 72 h. Yield was 63.79g, 84%. ^{31}P NMR: 19.2 ppm (s); ^{1}H NMR: 4.1 ppm (b), 3.6 ppm (t), 3.4 ppm (s), 1.3 ppm (t); ^{13}C NMR: 71.9 ppm, 67.6 ppm, 65.4 ppm, 62.5 ppm, 59.4 ppm, 16.5 ppm.

Results and Discussion

<u>Synthesis of the Additives</u>

Phosphazenes were chosen to investigate as novel additives for electrolytes for a number of reasons. First, it is known that polyphosphazenes were solid electrolytes that showed some of the best lithium ion conductivities and that these types of compounds had excellent lithium salt separation and chemical compatibility with typical lithium salts ($LiPF_6$, $LiClO_4$, etc.). (10) Therefore it was logical to investigate the small molecule analogues to the polyphosphazenes, namely trimeric phosphazenes. Second, these small molecule trimers exhibit simultaneously several beneficial properties desirable in electrolyte formulations.   They are non-flammable, non-volatile, non-toxic, voltage tolerant up to and beyond 5 volts, and have been found to be chemically compatible with all common materials of battery construction. This includes a host of commercially available anode materials (carbon, LTO, etc.), cathode materials (NMC, LNMO, etc.) and separator materials. Additionally it was discovered that they are fully miscible with a

host of conventional electrolytes such as EC, EMC, DMC, etc. and blends of these solvents.

The decision to investigate phosphazenes that possessed short chain ether groups was made because they were synthetically accessible, easily purified, and easily dried as they are non-volatile. Further, they posses all the beneficial properties enumerated above. In order to study these compounds, they first had to be synthesized as they are not commercially available. The phosphazene synthesis began with a starting phosphazene core, hexachlorocyclotriphosphazene. Sodium hydride was used to convert the starting alcohols to the corresponding alkoxides, using Shlenk synthetic techniques. The starting phosphazene was introduced to the reaction flask and a nucleophilic displacement of the chlorides was effected. Reaction progress was conveniently monitored by ^{31}P NMR. When the reaction was complete, purification was accomplished by a simple extraction washing procedure yielding the compound in high yield. A series of seven total compounds was synthesized, purified and dried. The composition of the pendant groups on each phosphazene compound is given in Figure 1.

Table 1. Structural formulations of the SM series of phosphazene additives.

Formulation	%	OR
SM-0	100	-O-CH₂CH₂-O-CH₂CH₂-O-CH₃
SM-1	38	-O-CH₂CH₂CH₂-O-CH₂CH₂-O-CH₃
	62	-O-CH₂CH₂-O-CH₃
SM-2	69	-O-CH₂CH₂CH₂-O-CH₃
	31	-O-CH₂CH₂-O-CH₃
SM-3	37	-O-CH₂CH₂-O-CH₃
	63	-O-CH₂-O-CH₃
SM-4	14	-O-CH₂CH₂-O-CH₃
	86	-O-CH₂-O-CH₃
SM-5	21	-O-CH(CH₃)CH₃ (isopropyl)
	79	-O-CH₂CH₂-CH₃
SM-6	69	-O-CH(CH₃)CH₃ (isopropyl)
	31	-O-CH₂-CH(CH₃)CH₃
SM-7	100	-O-CH₂CH₃
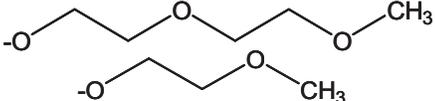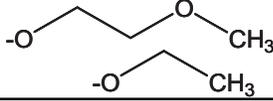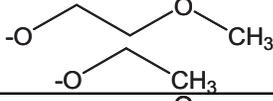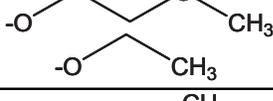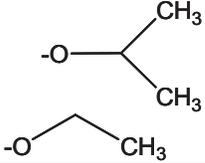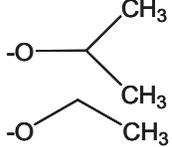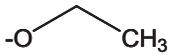
The initial prototype compound, SM-0 was synthesized with longer pendant arms on the phosphazene core as sufficient lithium salt solubility was a concern. Unfortunately

the viscosity was found to be unacceptably high. As a consequence of this discovery, the decision was made to synthesize a series of related compounds, SM-1 through SM-7 with successively smaller pendant groups to lessen the molecular weight and molecular size, reducing viscosity. This approach was successful as demonstrated by the viscometry results for both the pure compounds as well as the salted (with $LiPF_6$) formulations as shown in Table 2. Fortunately, the room temperature saturation concentration of $LiPF_6$ did not appreciably change with this shortening of the pendant groups, achieving a benefit in viscosity without sacrificing salt solubility.

Table 2. Viscosity of the pure and salted phosphazene compounds.

Formulation	Viscosity neat (cP)	Viscosity sat. w/LiPF6 (cP)
SM-0	75	1030
SM-1	58	605
SM-2	39	1750
SM-3	27	640
SM-4	21	260
SM-5	18	45
SM-6	14	38
SM-7	12	31

Physical Property Measurement of the Phosphazenes as Additives

Even with the benefit of lowered viscosity, initial coin cell tests revealed that these compounds were still too viscous to serve as a pure solvent for lithium ion batteries. It was then that the investigation of these compounds as co-solvents (35-75%) and additives (1-30%) was initiated. Blends were made with a conventional electrolyte at 5, 10, 20 and 30 % and the resulting electrolyte formulations studied and compared to the baseline conventional electrolyte. The first of these analyses was a study of the effect of the additives on electrolyte viscosity. As expected, the viscosity of the electrolytes rose linearly with increasing percentage of additive in the blend, as shown in Figure 1. However this rise in viscosity was minor, resulting in only an increase of as much as ~3 cP at the highest level studied 30%. It was also noted that the smaller and lighter additives produced less of a viscosity increase than the larger ones, with an increase of only ~1 cP. This was seen as a positive outcome for the promise of employing these as additives.
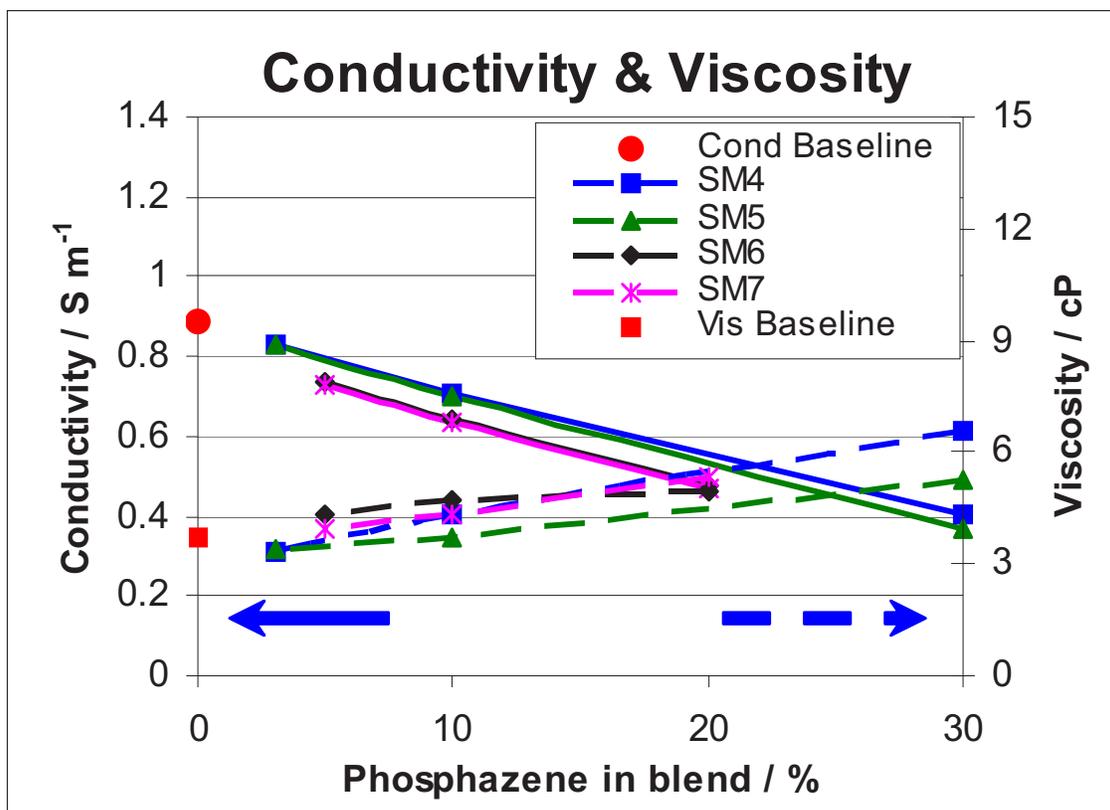
Figure 1. Comparison of conductivity and viscosity when INL phosphazenes are used as an additive to a conventional electrolyte.

A similar study was performed on the effects of the phosphazene additives in blends on the conductivity of the electrolyte. Again, the expected result was obtained in that a linear trend of lower conductivity was observed with increasing amounts of additive in the electrolyte. Similar to what was observed in the viscosity study, the effect was minor. The drop in conductivity went from ~0.9 S/m in the pure baseline electrolyte to ~0.4 S/m at the highest level studied (30%). Converse to the trends seen in viscosity, the lighter additives lowered the conductivity more than the larger heavier ones. This is attributed to the fact that the larger additives possess more oxygen ion carriers than the smaller ones, therefore lessening the impact on ion conductivity.

The next study that was performed was to investigate the effect of the additives on the flash point of the electrolyte blends. As the phosphazenes are non-volatile and non-flammable it was expected that adding these compounds to the electrolyte would have a positive benefit. That was indeed the observed trend. As shown in Figure 2, the flash point was raised roughly linearly with increasing amounts of additive. With 30% of the additive incorporated into the formulation, the flash point was raised by ~5 °C. The trend observed by comparing the various additives was that the smaller additives had a more pronounced effect in raising the flash point than the larger ones. This is attributed to the fact that the smaller ones have a more inorganic character owing to their shorter pendant groups.
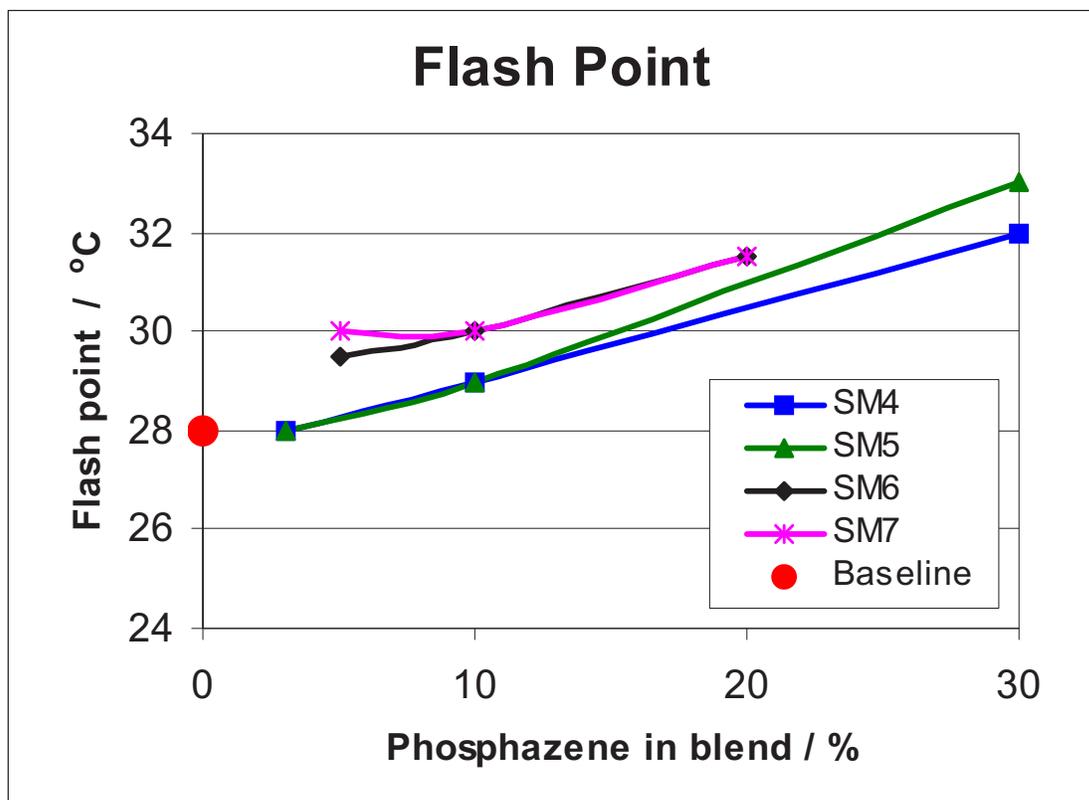
Figure 2. Effect of the INL phosphazene additives on the flash point of the electrolytes.

Thermal Behavior of Electrolytes with the Additives

It was well known that the phosphazene additives were extremely thermally stable. The typical onset of thermal degradation is approximately 270 °C. It was expected that the incorporation of these additives into the electrolyte formulations would impart some benefit.   To investigate the magnitude of the benefit a thermolysis experiment was performed.   Several vessels were loaded with the baseline conventional electrolyte accompanied with baseline plus additives, SM-4 and SM-5 at 10% and 30% loading. The vessels were sealed and removed from the argon glovebox where the formulations were made. They were placed into a thermal chamber set to 60 °C and allowed to remain for 60 days undisturbed. Periodically, they were examined and photographed. As expected, the baseline electrolyte rapidly degraded, visibly discoloring within the first two weeks. By the end of the 60 day study period, the baseline was extremely degraded as evidenced by changes in the color as shown in Figure 4. In addition to the discoloration, the baseline had partially solidified yielding a highly viscous solution with approximately half or more of the volume having solidified into large black masses. In stark contrast, the formulations that contained the additives exhibited little to no evidence of degradation whatsoever. In addition to resisting thermal degradation by the additives themselves, they also protected the baseline from thermal degradation. As this was a surprising result, this experiment was repeated using different phosphazene additives and in the second experiment a much lower amount of additive was used, at levels of 1, 3, 5, 10, and 20%. Again, the results were the same. The baseline rapidly degraded yielding a discolored, semi-solid mass as shown in Figure 5.   The electrolytes that contained additive, in amounts as little as 1%, were completely unchanged (see caveat for SM-7 in Fig. 5). All

of the formulations from both studies have been stored in an argon glovebox and multi-dimensional NMR experiments are ongoing to investigate the mechanism of this protecting effect that the additives have demonstrated.


A: 10% SM4   E: 10% FM1
B: 30% SM4   F: 30% FM1
C: 10% SM5   G: Baseline
D: 30% SM5

All tests at 60 °C.   Baseline is 1.2M LiPF$_6$ in EC/EMC (2:8)
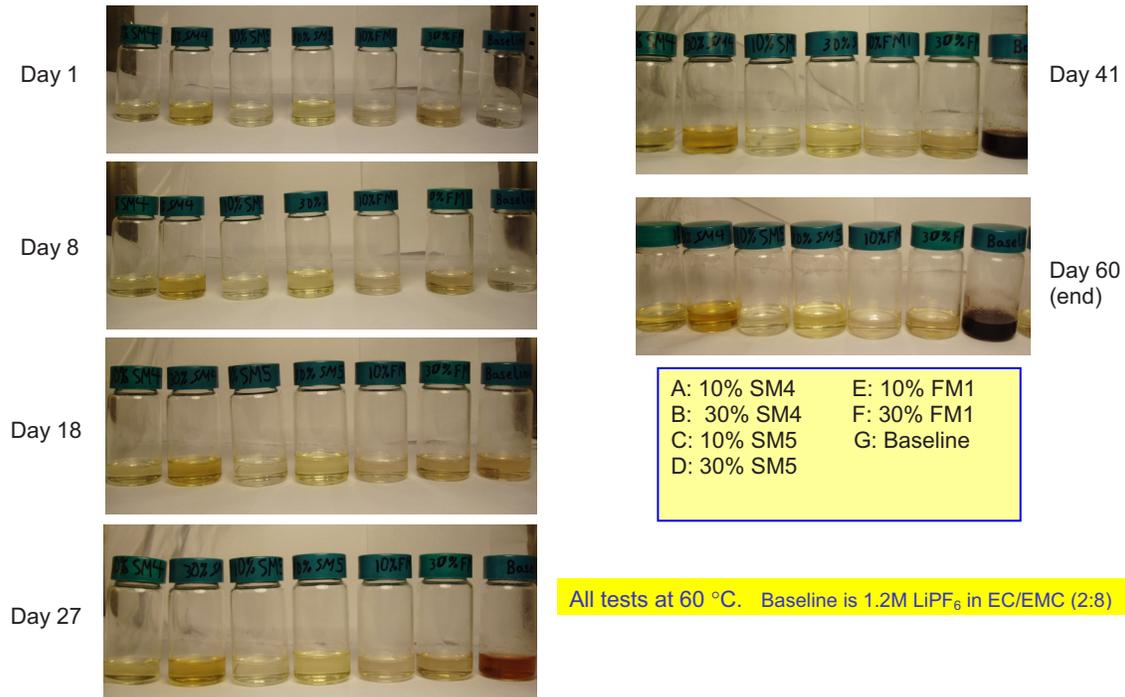
Figure 4. First thermolysis experiment.

A: Baseline   E: 10% SM6   I: 5% SM7
B: 1% SM6   F: 20% SM6   J: 10% SM7
C: 3% SM6   G: 1% SM7   K: 20% SM7
D: 5% SM6   H: 3% SM7

CONCLUSION:
The presence of INL phosphazene SM6 has a profound effect in stabilizing the baseline electrolyte at levels as low as 1%. SM7-doped samples discolor due to 40 ppm water contamination; SM7 study will be repeated.

All tests at 60 °C.   Baseline is 1.2M LiPF$_6$ in EC/EMC
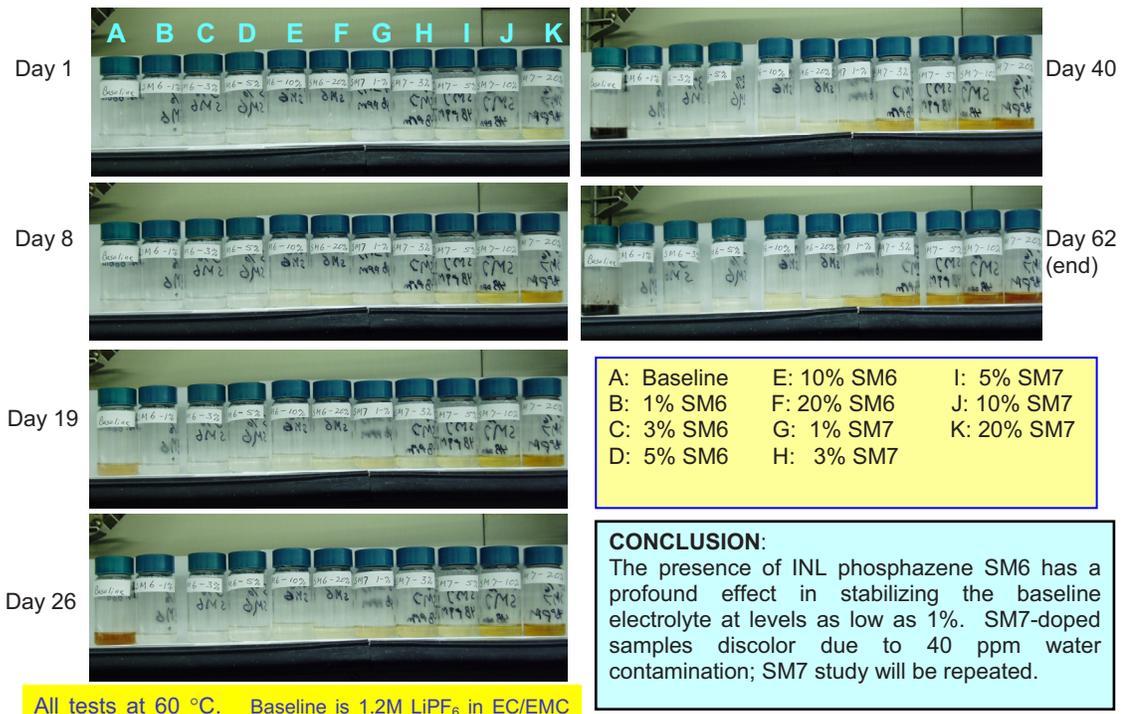
Figure 5. Second thermolysis experiment.

Electrochemical Characterization

Figure 6 depicts potentiodynamic curves obtained for five electrolytes: the baseline electrolyte and the baseline blended to contain 20% SM-4, SM-5, SM-6, and SM-7. Ni metal was used as the working electrode at voltages negative to OCV, while Al metal was used positive to OCV. Li metal served as both the counter and reference electrodes. The stable electrochemical window (EW) is observed here as the range of potentials in both directions from OCV where currents are extremely low (less than 1–2_μcm^{-2}) where significant reduction or oxidation processes are not present. There are a number of methods and definitions, described in the open literature, as to how to characterize and measure the electrochemical window. All of these methods are relative and based on key assumptions. Our measurements are sufficiently accurate to see meaningful differences in the five electrolytes. Figure 6 shows that the phosphazene additives do significantly increase the electrochemical window. For the baseline electrolyte alone, the window is measured to be 0.79V. Upon incorporation of the additives, this window significantly increases to as much as 1.79V, adding a full volt of stability to the electrolyte formulation. This also indicates that there are some beneficial interactions between control electrolyte components and the phosphazene additives.
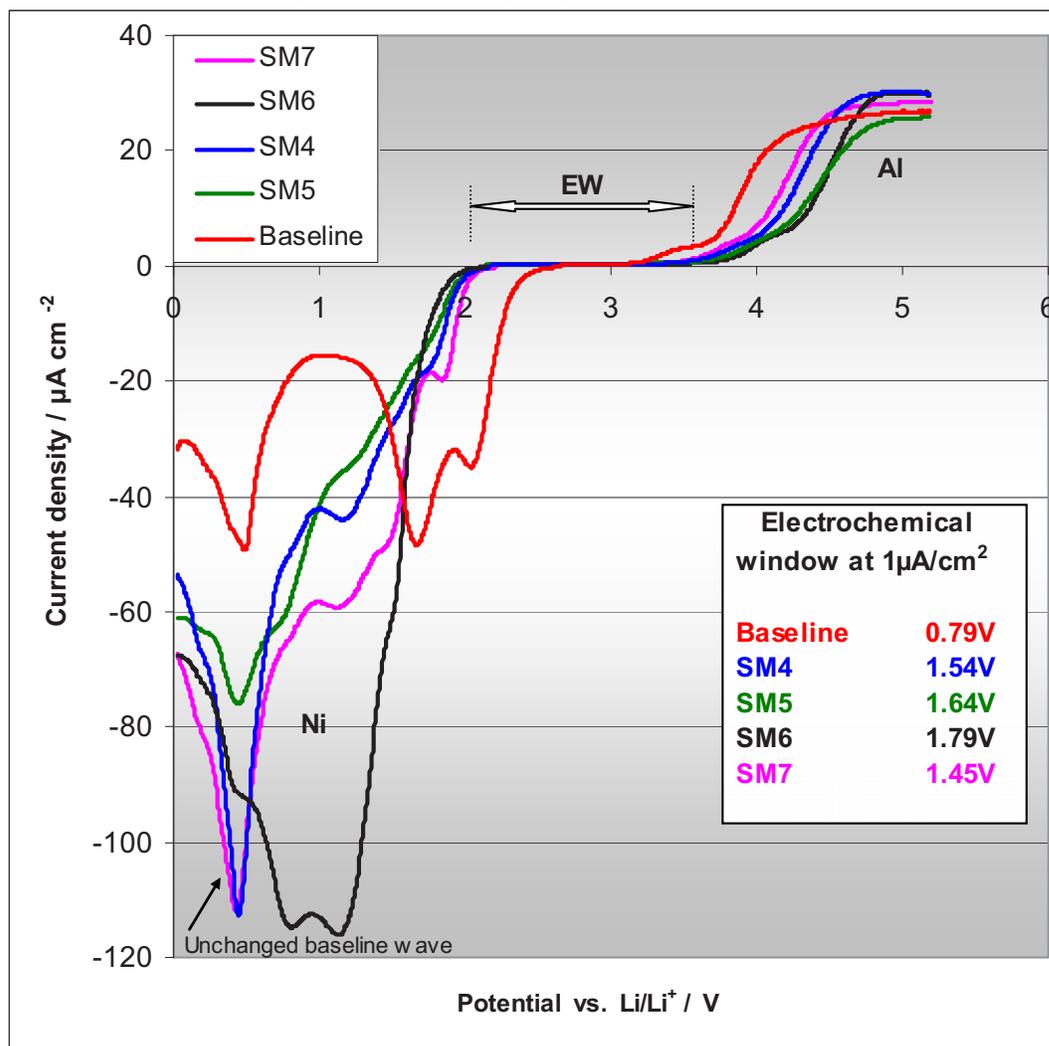

Figure 6. Voltamagram of the baseline with and without additives.

Coin Cell Testing

To complete this study of these phosphazene additives, coin cell batteries were fabricated using the pure baseline electrolyte as well as electrolyte formulations incorporating 3 and 10% of the additives. Two different electrode pair combinations were employed, lithiated nickel manganese oxide (LNMO) paired with lithium titanium oxide (LTO) and nickel manganese cobalt oxide (NMC) paired with carbon. The cells were formed at a C/10 rate for three cycles with a two hour rest between cycles. Then the cells were cycled at increasing rates; 5 cycles at C/10, C/3, 1C, followed by 20 cycles at 3C, followed by two more cycles at a C/10 rate with no rest time between cycles. All testing was performed in a thermal chamber at 30 °C. The capacity data are shown in Figures 7 and 8. For the cells employing the LNMO/LTO pair, the capacities are slightly lower even at the slowest cycling rates. At the highest rate, the capacity difference compared to the pure baseline electrolyte becomes more significant. Cell polarization is evident, especially at the highest cycling rate, and this becomes more pronounced with higher loading levels of the additive. However, upon the return to the C/10 rate at the end of the testing, the final C/10 capacities are equal to or even higher than after initial formation, giving evidence of little to no cell aging. The performance of the additives was significantly better in the NMC/Carbon cells. At the lower rates, the cells with the additives are nearly identical to that observed in the pure baseline. Even at the highest rate (3C) the cells containing the additive are only slightly below that observed for the baseline electrolyte. Upon the return to the C/10 rate and the end of the testing, the cells with additive return to being identical to the baseline electrolyte with all cells exhibiting a capacity slightly lower than that observed right after formation.
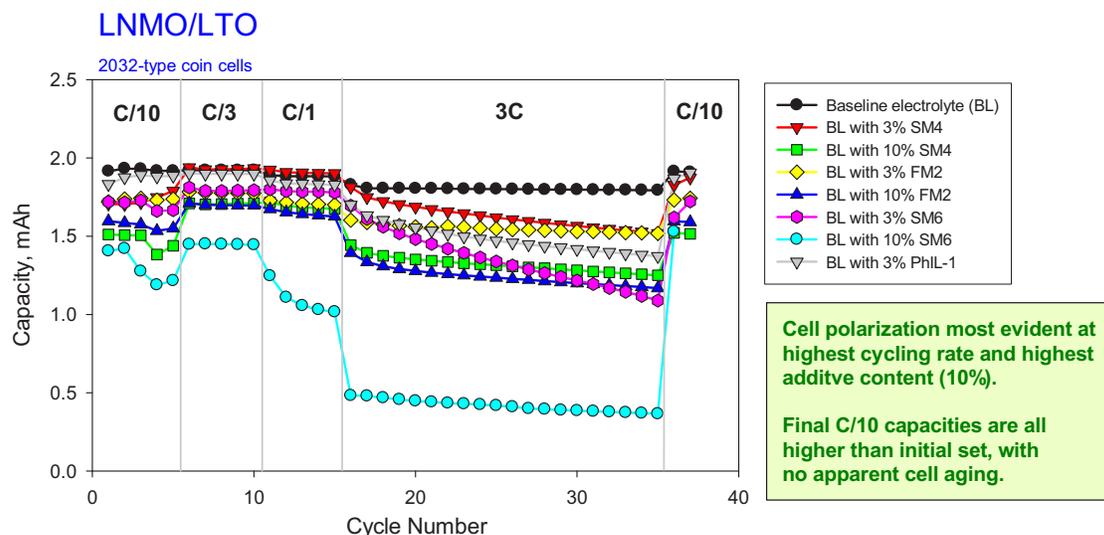

Figure 7. Capacity data for cells with and without phosphazene additives for the LNMO/LTO electrode pair.

NMC/Carbon

2032-type coin cells

These are updated results using calandered electrode materials from SNL.

- ● Baseline electrolyte (BL)
- ▼ BL with 3% SM4
- ■ BL with 10% SM4
- ◆ BL with 3% FM2
- ▲ BL with 10% FM2
- ⬠ BL with 3% SM6
- ○ BL with 10% SM6
- ▽ BL with 3% PhIL-1

Cell polarization is higher, probably due to impedance tied to EIS HF arc. Final C/10 capacities are slightly lower than initial set.

All additives yield similar cell performance, with only subtle differences noted between the 3 & 10% cells, and at each rate.

Figure 8. Capacity data for cells with and without phosphazene additives for the NMC/Carbon electrode pair.

Modeling of Additive/Lithium Binding (Ion Solvation)

All geometry optimizations and vibrational analyses were performed with the Gaussian03 program (11). For consistency, both neutral and cationic species were calculated using density functional theory (12) at the B3LYP/6-311++G(d,p) level of theory (13, 14). All calculated structures are true minima, *i.e.* no imaginary frequencies.


a   b
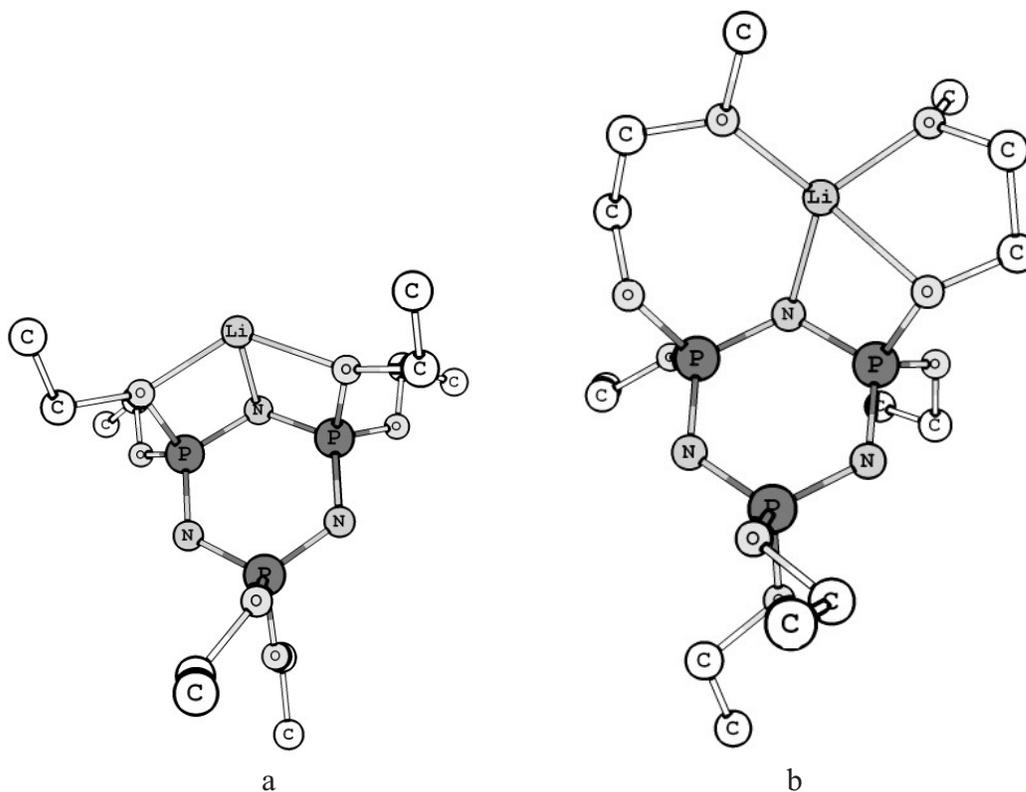
Figure 9. a) SM-7, b) SM-3 with ether oxygens bonding to Li$^+$.

The lithium adducts of phosphazenes SM-3 through SM-7 were modeled using the closest approximation to the pendant group distributions listed in Table 1. Figure 9 illustrates the bonding in these systems. In Figure 9a, the lithium is bonded to the two adjacent oxygens, both attached to the ring, and the ring nitrogen. In the simpler phosphazenes, without long pendant groups containing ether linkages, this is the most stable position for the lithium. This pocket structure for the lithium has been discussed previously for polyphosphazenes. (15, 16) When longer pendant groups are present, the ether oxygens can bond to the lithium, as shown in Figure 9b. This bonding environment around the lithium is consistent with previous reports. (15, 16) Nitrogen has a higher binding energy than oxygen, by 12.3 kcal/mol, (16) thus the preferred position for Li^+ is next to the phosphazene ring.

Table 3 lists the lithium binding energies for the phosphazenes. In the simpler, three coordinate bonding environment shown in Figure 3a, the binding enthalpies are all roughly 75 kcal/mol. When the ether oxygens bond to Li+, the binding enthalpy increases to 92.4 kcal/mol, an increase of nearly 20 kcal/mol. (SM-3*) The pendant groups are flexible enough that steric strain is not an issue, allowing the ether oxygens to bond to Li^+ without raising the overall energy, which would decrease the binding enthalpy. Also, the ring structures created by lithium coordination will certainly affect the energy. In Figure 9a, two 4-membered rings are created, which are sterically unfavorable. In Figure 9b, one 4-membered ring is present, along with sterically more favorable 5- and 7-membered rings, which will lower (with respect to 4-membered rings) the overall energy and increase the binding enthalpy.

Table 9. Lithium binding enthalpies for SM compounds

Compound	Binding Enthalpy (kcal/mol)
SM-3*	92.4
SM-3	72.2
SM-4	75.7
SM-5	74.2
SM-6	75.6
SM-7	74.7

Conclusions

A series of novel phosphazene additives was synthesized, characterized and electrochemically studied, including fabrication of coin cells. These additives imparted several beneficial properties to the baseline electrolyte. First, they caused a minimal increase in viscosity with a concomitant minimal drop in conductivity. Incorporation of these additives also drove a rise in the flash point of the electrolyte formulations, potentially increasing the safety of batteries that include these additives. More importantly, use of these additives significantly increased the electrochemical window, providing a stabilizing effect on the electrolyte. Of even greater significance, these additives imparted a dramatically increased thermal stability to the organic components of the electrolyte. Finally, DFT modeling has been used to look at lithium additive interactions to aid in the design of future additives. Overall, phosphazenes continue to exhibit promise as additives for the current generation of electrolytes.

Acknowledgments

References

1. *Advances in Lithium-Ion Batteries*, W. A. Van Schalkwijk and B. Scrosati, Editors, Kluwer Academic, New York (2002).
2. Y. Watanabe, S. Kinoshita, S. Wada, K. Hoshino, H. Morimoto, S. Tobishima, *J. Power Sources*, **179**(2), 770 (2008).
3. A. Balducci, S. Jeong, G. Kim, S. Passerini, M. Winter, M. Schmuck, G. Appetecchi, R. Marcilla, D. Mecerreyes, V. Barsukov, V. Khomenko, I. Cantero, I. De Meatza, M. Holzapfel, N. Tran, , *J. Power Sources*, **196**(22), 770 (2011).
4. J. Goodenough and Y. Kim, *Chem. Mater.*, **22**, 587 (2010).
5. T. Hirai, I. Yoshimatsu, J. Yamaki**,** *J. Electrochem. Soc.,* **141**(9), 2300, (1994).
6. C. Chang, S. Hsu, Y. Jung, C. Yang, *J. Power Sources*, **196**, 9605 (2011).
7. Young-Gi Lee and Jaephil Cho, *Electrochimica Acta* **52** 7404, (2007).
8. S. Dalavi, M. Xu, B. Ravdel, L. Zhou, B. Lucht**,** *J. Electrochem. Soc.,* **157**(10) A1113-A1120 (2010).
9. M. Xu, L. Zhou, L. Hao, L. Xing, W. Li, B. Lucht, *J. Power Sources*, **196**, 6794, (2011).
10. P. Blonsky, D. Shriver, P. Austin, H. Allcock, *J. Am. Chem. Soc.*, **106**(22), 6854, (1984).
11. Gaussian 03, Revision C.02, M. J. Frisch, et al., Gaussian, Inc., Wallingford CT, (2004).
12. R. Parr, W. Yang, Density Functional Theory of Atoms and Molecules, Oxford University Press, New York (1989).
13. A. Becke, *Phys. Rev. A* **38**, 3098 (1988**)**.
14. C. Lee, W. Yang, R. Parr, *Phys. Rev. B* **37**, 785 (1988**)**.
15. T. Luther, F. Stewart, J. Budzien, R. LaViolette, W. Bauer, M. Harrup, C. Allen, A. Elayan, *J. Phys. Chem. B* **107**, 3168 (2003).
16. Y. Wang, P. Balbuena, *J. Phys. Chem. B* **108**, 15694 (2004).